QCD thermodynamics with nonzero chemical potential at $N_t = 6$ and effects from heavy quarks

C. DeTar and L. Levkova

Physics Department, University of Utah, Salt Lake City, Utah 84112, USA

Steven Gottlieb *

Department of Physics, Indiana University, Bloomington, Indiana 47405, USA

U.M. Heller

American Physical Society, One Research Road, Ridge, New York 11961, USA

J.E. Hetrick

Physics Department, University of the Pacific, Stockton, California 95211, USA

R. Sugar

Department of Physics, University of California,

Santa Barbara, California 93106, USA

D. Toussaint

Department of Physics, University of Arizona, Tucson, Arizona 85721, USA

(Dated: June 30, 2010)

Abstract

We extend our work on QCD thermodynamics with 2+1 quark flavors at nonzero chemical potential to finer lattices with $N_t = 6$. We study the equation of state and other thermodynamic quantities, such as quark number densities and susceptibilities, and compare them with our previous results at $N_t = 4$. We also calculate the effects of the addition of the charm and bottom quarks on the equation of state at zero and nonzero chemical potential. These effects are important for cosmological studies of the early Universe.

PACS numbers: 12.38.Gc, 12.38.Mh, 25.75.Nq

* On sabbatical leave at NCSA, University of Illinois, Urbana IL 61801, USA

I. INTRODUCTION

The quark-gluon plasma (QGP) is a state of matter which forms at very high temperatures or densities. It is believed that up to microseconds after the big bang the QGP was a dominant component of the Universe. This state of matter is recreated in heavy-ion collision experiments [such as are done at the Relativistic Heavy Ion Collider (RHIC)] which study its formation and transition to ordinary matter. The equation of state (EOS) of the QGP is essential to our understanding of its hydrodynamic expansion and consequently of the particle spectra produced in these experiments. We have studied the EOS at zero and nonzero chemical potential previously [1, 2]. Here we extend our work in two directions. (1) We present results for the EOS at nonzero chemical potential at finer lattice spacings than our previous work. Here the temporal lattice extent is $N_t = 6$, where previously it was $N_t = 4$. Preliminary results for the $N_t = 6$ case were reported in Ref. [3]. It is important to compare the two cases and determine the size of the discretization error as a step towards taking the continuum extrapolation. (2) We include the effects of the charm and bottom quarks. A preliminary progress report on the charm quark effects was given in Ref. [4]. We use the heavy-quark-quenched approximation. That is, the charm and bottom quarks appear as valence quarks, but not as dynamical sea quarks. Thus we ignore all charm and bottom quark loops contributing to the operators we determine in order to obtain the EOS. This approximation introduces an error in our calculation. However, considering that the charm and bottom quarks are much heavier than our sea u, d, and s quarks, it seems plausible that adding sea charm and bottom quarks would have a small effect for temperatures much less than their masses. Still, until we have a dynamical c- and b-quark calculation to compare against, this statement remains a conjecture. The equation of state with the charm and bottom quarks added is most applicable to the study of the early Universe, since the time scale relevant to the heavy-ion collisions at RHIC is probably too short for the charm and bottom quarks to thermalize and have a visible effect on the particle data.

As in our previous $N_t = 4$ determination of the EOS at nonzero chemical potential, we employ the Taylor expansion method. For a detailed description of the method, see Refs. [5, 6]. The expansion is carried up to sixth order in the expansion parameters μ_q/T, where μ_q is the chemical potential for a certain quark flavor q and T is the temperature.

The gauge ensembles we used in this work are the same as in Ref. [2]. They are generated using the asqtad improved staggered action [7] and have two degenerate light quarks and a strange

quark in the sea. The ensembles lie approximately on a trajectory of constant physics, where the strange quark mass m_s is tuned to be close to its physical value, and the light quark mass m_l is one-tenth of m_s. Because in this paper we also consider charm and bottom quarks, we do not refer to the strange quark as the "heavy quark" as in Refs. [1, 2].

In Sec. II, we present our results for the 2+1 flavor EOS with nonzero chemical potential at $N_t = 6$, and compare it with our previous one at $N_t = 4$. We also show other thermodynamic quantities, such as the quark number susceptibilities and light-quark density. Section III gives our findings for the isentropic EOS for 2+1 flavors. In Sec. IV, we calculate the effects of the charm quark on the EOS at zero and nonzero chemical potential, using the heavy-quark-quenched approximation to represent it. Section V does the same for the bottom quark. In Sec. VI, we give our conclusions. The Appendixes contains some helpful formulas for the application of the Taylor expansion method for the EOS calculation in the 2+1+1 quark flavor case.

II. THE EOS AT NONZERO CHEMICAL POTENTIAL AT $N_t = 6$ FOR 2+1 FLAVORS

The Taylor expansion method allows us to represent the pressure p and the interaction measure I in the case where both the light and the strange quark chemical potentials are nonzero, as the following infinite sums:

$$\frac{p}{T^4} = \frac{\ln \mathcal{Z}}{T^3 V} = \sum_{n,m=0}^{\infty} c_{nm}(T) \left(\frac{\bar{\mu}_l}{T}\right)^n \left(\frac{\bar{\mu}_s}{T}\right)^m, \tag{1}$$

$$\frac{I}{T^4} = -\frac{N_t^3}{N_s^3} \frac{d \ln \mathcal{Z}}{d \ln a} = \sum_{n,m}^{\infty} b_{nm}(T) \left(\frac{\bar{\mu}_l}{T}\right)^n \left(\frac{\bar{\mu}_s}{T}\right)^m. \tag{2}$$

In the above, $\bar{\mu}_{l,s}$ are the chemical potentials for the light and strange quarks in physical units, T is the temperature, N_s is the spatial lattice extent, $\mathcal{Z}$ is the partition function and a is the lattice spacing. Because of CP symmetry, the expansion coefficients c_{nm} and b_{nm} are nonzero only if $n+m$ is an even integer. The explicit forms of these coefficients are given in Ref. [2], and since they are somewhat involved, we do not repeat them here. We calculate the coefficients stochastically with random Gaussian sources. Inside the transition region, we used 800 random sources per lattice, and outside, 400. With these numbers, the stochastic error in the unmixed second order coefficients, *i.e.*, the diagonal quark number susceptibilities at zero chemical potential, is about 20% of the full statistical error. These coefficients are the ones with largest contribution to the thermodynamic quantities for each type of quark. For the fourth order unmixed coefficients, this

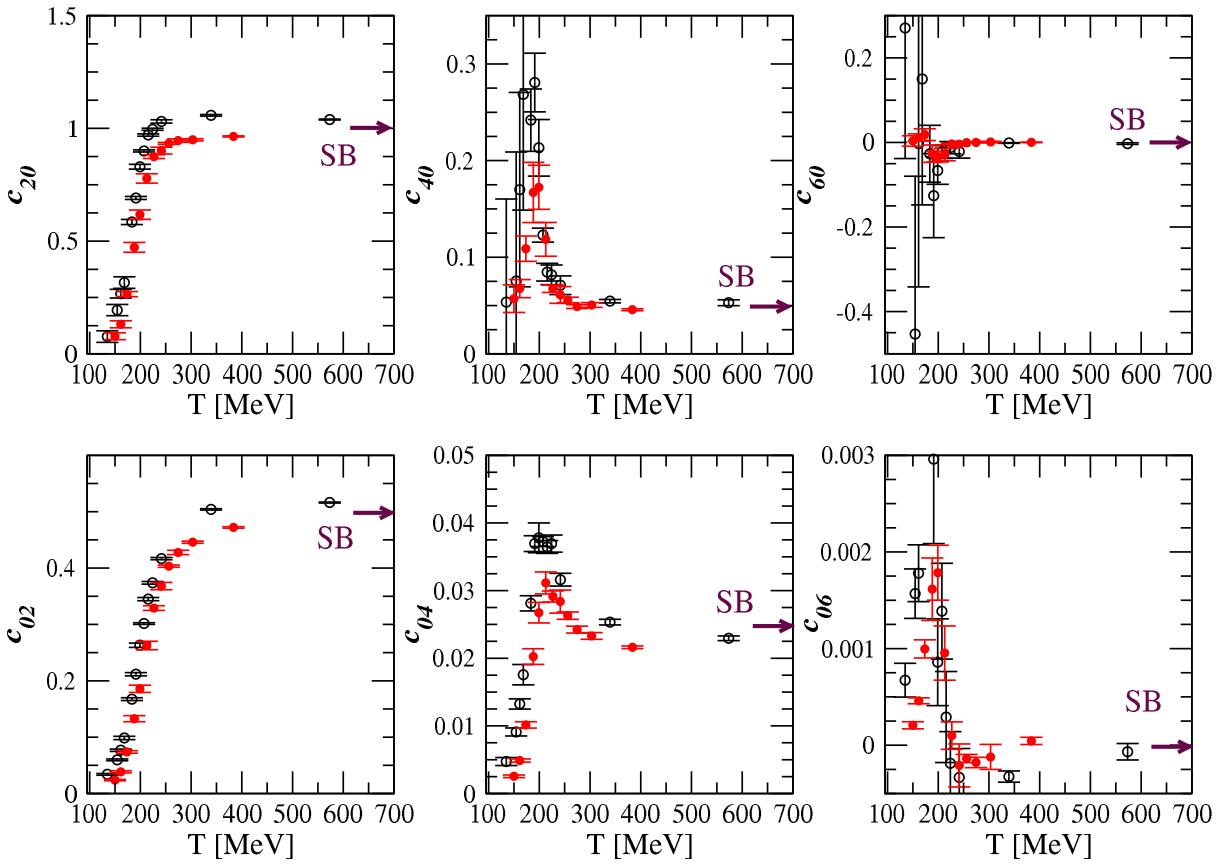

FIG. 1: Unmixed coefficients c_{n0} and c_{0n} in the Taylor expansion of the pressure as a function of temperature. The new results for $N_t = 6$ are shown in filled (red) circles; empty (black) circles are used for $N_t = 4$ (from Ref. [2]). Arrows indicate the Stefan-Boltzmann limit for each of the coefficients.

error is about 50% of the final error. For the rest of the coefficients (mixed coefficients and all coefficients of sixth order), the contribution of the stochastic error is dominant. A further increase of the number of sources as a way to decrease the stochastic noise seems impractical at this point. We need either significantly more computer power or a substantial improvement of the noisy estimators in order to reduce the resulting stochastic error.

Figures 1 and 2 show some of the coefficients in the pressure expansion and compare our new results at $N_t = 6$ (red filled circles) with the previous ones [2] at $N_t = 4$ (black empty circles). We can see that the errors for the $N_t = 6$ case are smaller than the ones at the shorter temporal extent, due to both the increased volume and increased number of random sources. (We previously used 100–200 sources.) There is also a shift in the central values between the two cases which indicates that the discretization effects at $N_t = 4$ are significant. The approach of the coefficients to the (massless) Stefan-Boltzmann continuum limit with increasing T in the case of $N_t = 6$ is slower,

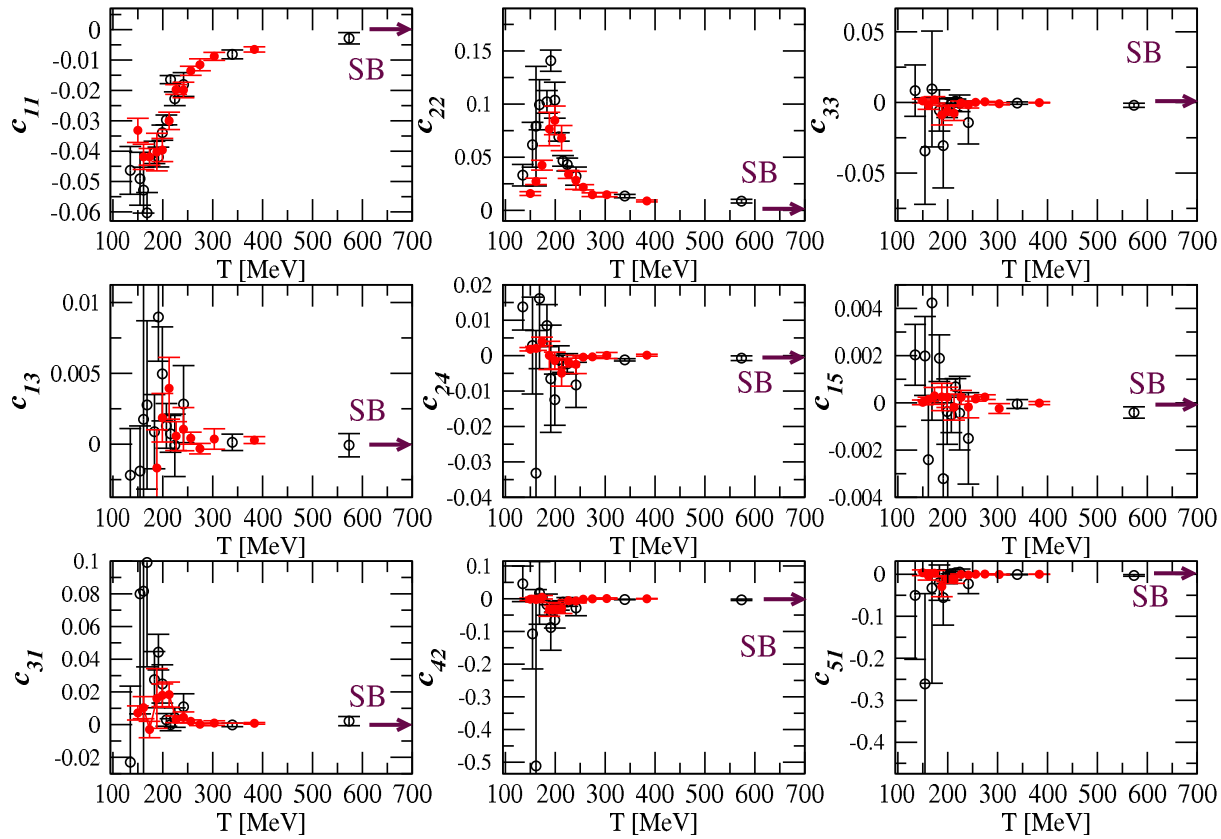

FIG. 2: Mixed coefficients c_{nm} in the Taylor expansion of the pressure as a function of temperature. The new results for $N_t = 6$ are shown in filled (red) circles; empty (black) circles are used for $N_t = 4$ (from Ref. [2]). Arrows indicate the Stefan-Boltzmann limit for each of the coefficients.

and the structure at low temperature is made somewhat clearer due to the smaller errors on the data. Similarly, Figs. 3 and 4 compare the unmixed and mixed coefficients b_{nm} involved in the Taylor expansion of the interaction measure at the two different temporal extents. These coefficients are calculated independently from the ones in the pressure expansion (although the two sets of coefficients are technically related by integration). The operators involved in the determination of the interaction measure expansion coefficients are intrinsically noisier, which is reflected in the larger errors on the data. Still, the shift in central values and errors in the b_{nm} coefficients in going from $N_t = 4$ to 6 is qualitatively similar to that of the pressure coefficients c_{nm}.

Having obtained the coefficients in the Taylor expansions in Eqs. (1) and (2), we can now turn to calculating the EOS. Because of the nonzero $c_{n1}(T)$ terms, a nonzero strange quark density n_s is induced even with $\mu_s = 0$. (We use μ_f to denote the chemical potential in lattice units for flavor f). To study the $n_s = 0$ plasma, we must, therefore, tune μ_s as a function of μ_l and T. Figures 5 (both

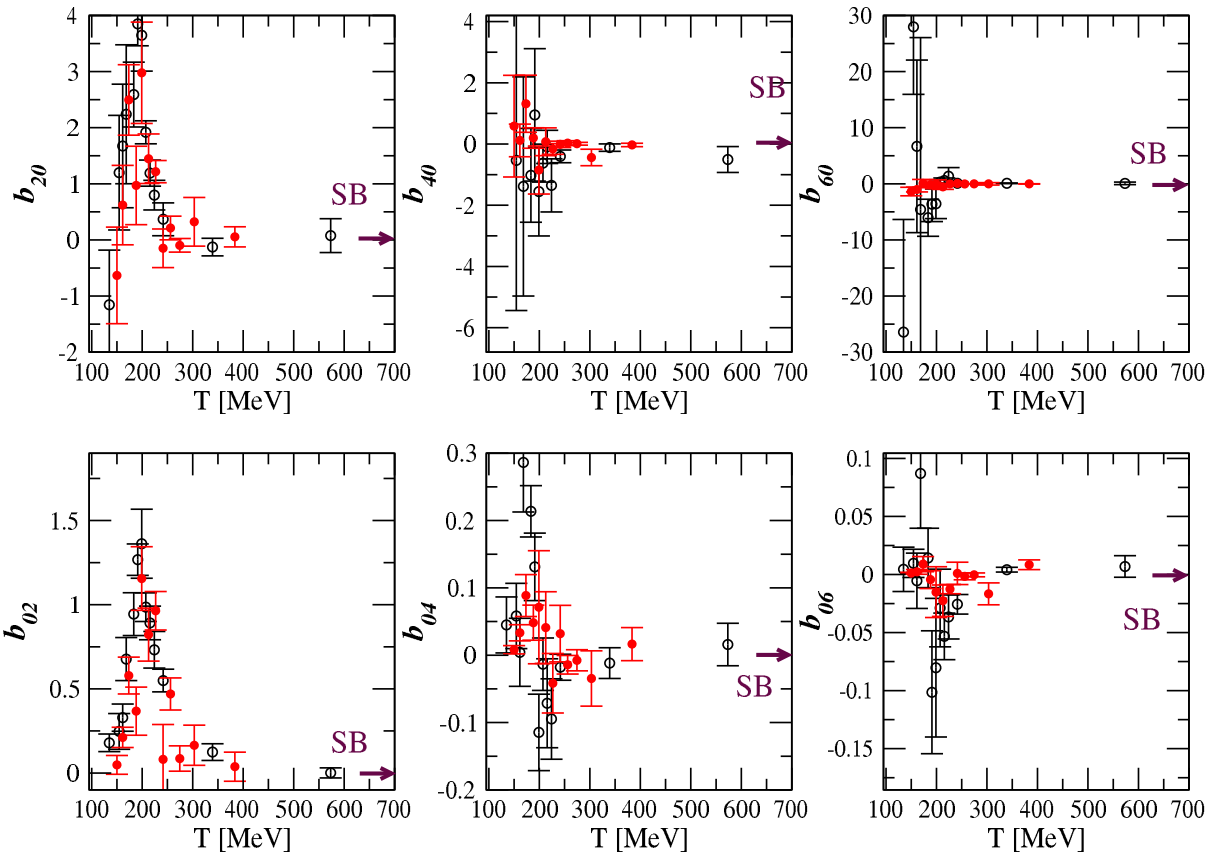

FIG. 3: Unmixed coefficients b_{n0} and b_{0n} in the Taylor expansion of the interaction measure as a function of temperature. The new results for $N_t = 6$ are shown in filled (red) circles; empty (black) circles are used for $N_t = 4$ (from Ref. [2]). Arrows indicate the Stefan-Boltzmann limit for each of the coefficients.

panels) and 6 (left panel) show the changes in the interaction measure (ΔI), pressure (Δp) and energy density ($\Delta\varepsilon = \Delta I + 3\Delta p$) at $\bar{\mu}_l/T = 0.1, 0.2, 0.4$, and 0.6, and with $\bar{\mu}_s/T$ tuned along the trajectory so that $n_s \approx 0$. We see statistically significant discretization effects when we compare the $N_t = 4$ and 6 cases for Δp, with the latter data lying lower than the former. The ΔI results have larger errors, and discerning differences in the data from the two temporal extents is more difficult. The $N_t = 6$ data is slightly but consistently lower than the one from the $N_t = 4$ calculation; however, this is not a statistically significant observation. The change in the energy density $\Delta\varepsilon$ inherits the large errors from ΔI, and the same conclusions apply for it. The discretization effects for the light-quark density (n_{ud}), the light-light and strange-strange quark number susceptibilities (χ_{uu} and χ_{ss}, respectively), are examined in Figs. 6 (right panel) and 7 (both panels). The effect of increasing the temporal extent from $N_t = 4$ to 6 is to lower these quantities by 4%–10%. For the range of values of $\bar{\mu}_l/T$ that we examine, we do not find any evidence for peaks that could presage critical

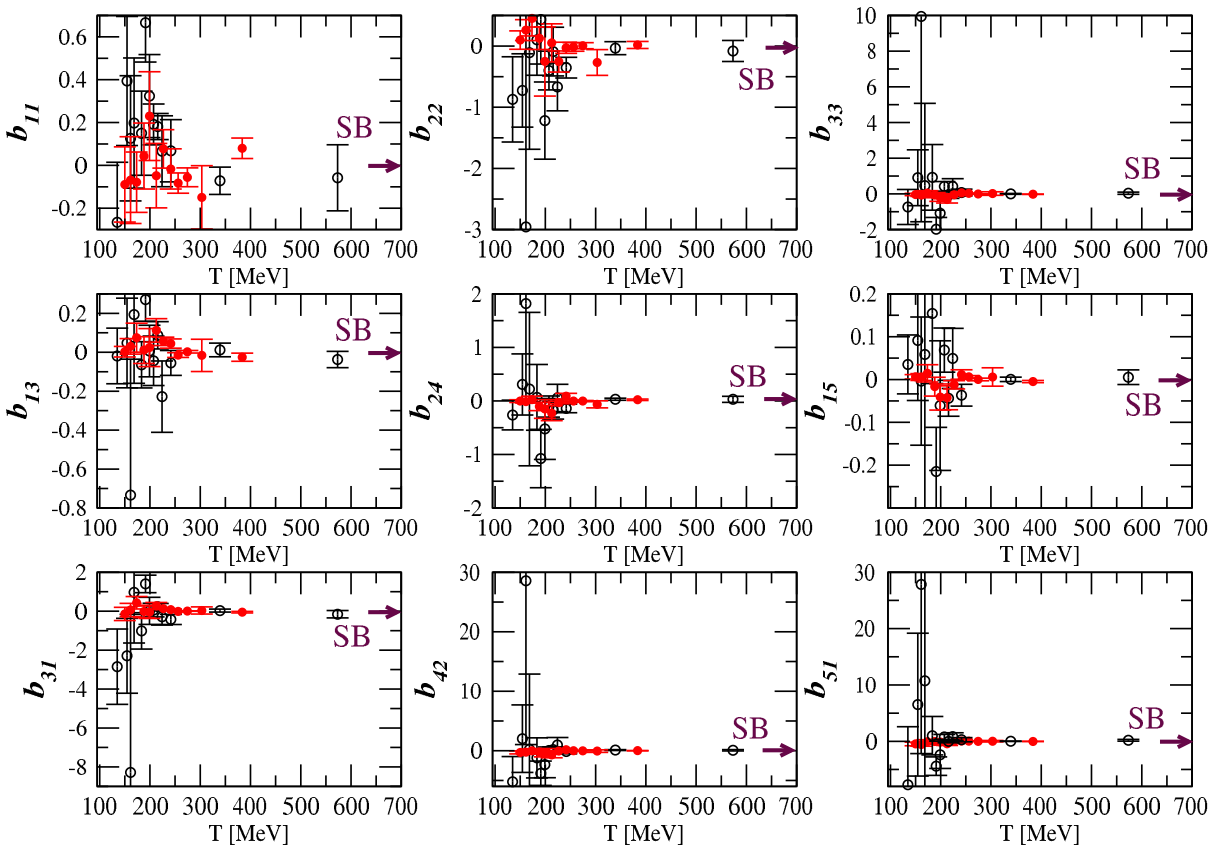

FIG. 4: Mixed coefficients b_{mn} in the Taylor expansion of the interaction measure as a function of temperature. New results for $N_t = 6$ are shown in filled (red) circles, empty (black) circles are used for $N_t = 4$ (from Ref. [2]). Arrows indicate the Stefan-Boltzmann limit for each of the coefficients.

behavior in χ_{uu}. The light-strange quark number susceptibility (χ_{us}), shown in Fig. 8 (left panel), is too noisy for a reliable conclusion about its discretization effects; there is only a hint at a possible move toward lower absolute values at the larger N_t.

III. THE ISENTROPIC EQUATION OF STATE

The form of the EOS most applicable to the experimental conditions of the heavy-ion collisions is the isentropic one. There, after thermalization, the system expands and cools with constant entropy. We determine the isentropic EOS by performing our calculations at fixed ratio of entropy to baryon number (s/n_B). This is achieved by finding the trajectories in the (μ_l, μ_s, T) space which satisfy (within errors) both $s/n_B = C$ and $n_s = 0$, where C is a constant whose value depends on the particular experiment we are interested in. For AGS, SPS, and RHIC, we have $s/n_B = 30$,

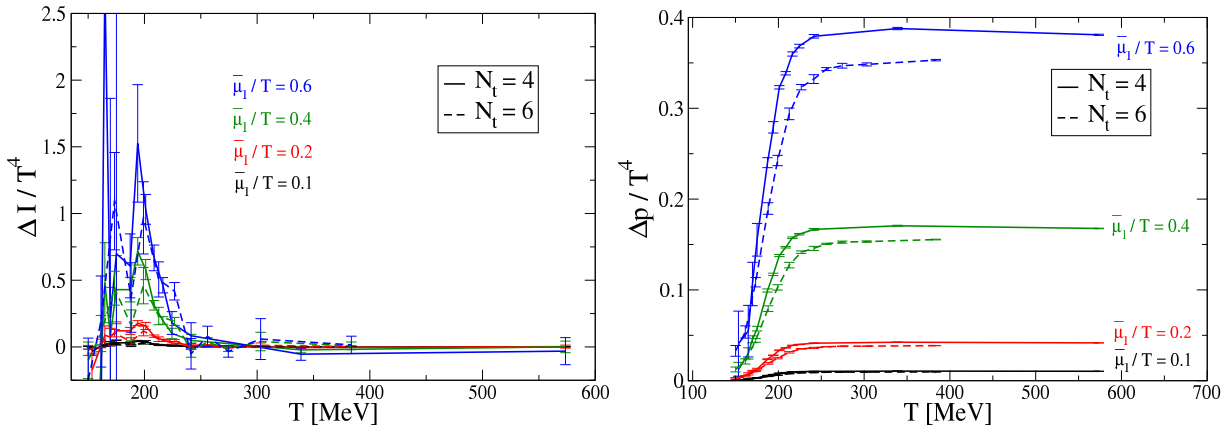

FIG. 5: (Left panel) The change in the interaction measure due to the nonzero chemical potentials *vs.* temperature. At a given N_t, the larger $\bar{\mu}_l/T$, the higher the data appears on the plot. (Right panel) Similarly, the change in the pressure.

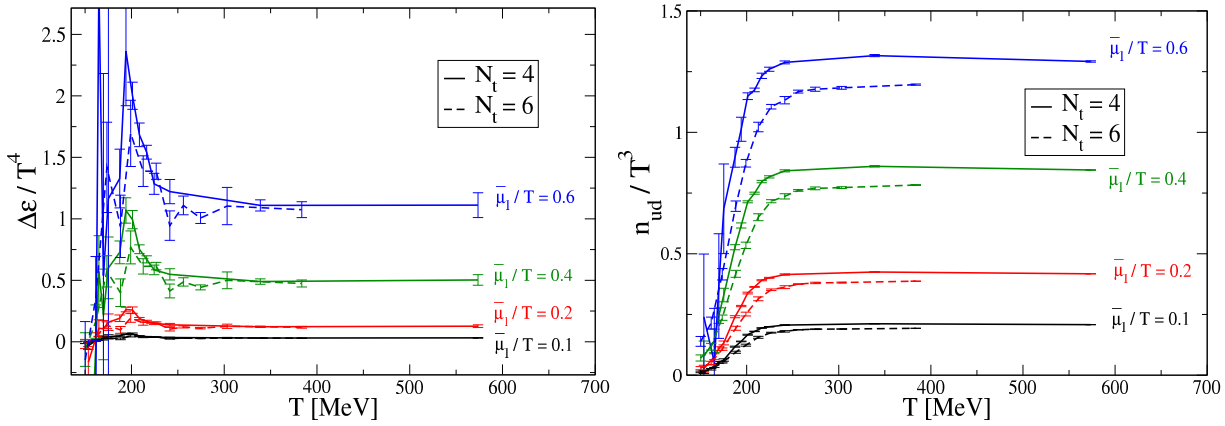

FIG. 6: (Left panel) The change in the energy density due to the nonzero chemical potentials *vs.* temperature. (Right panel) The light-quark density *vs.* temperature for several values of $\bar{\mu}_l/T$ (in different colors) and μ_s tuned such that $n_s \approx 0$.

45, and 300, respectively. Figures 8 (right panel) and 9 (both panels) show our results for the interaction measure, pressure, and energy density for the different s/n_B values appropriate for these experiments. We compare the new results at $N_t = 6$ (filled symbols) with the ones already published in Ref. [2] at $N_t = 4$ (empty symbols). For these three quantities, the comparison shows negligible effects due to the increase of the temporal extent N_t. The reason for this is that by far the largest contribution to these quantities—the zero-chemical potential (zeroth order) term in their respective Taylor expansions— does not show large discretization effects [1]. On the other hand, quantities which do not have a zeroth order term may show larger differences between the

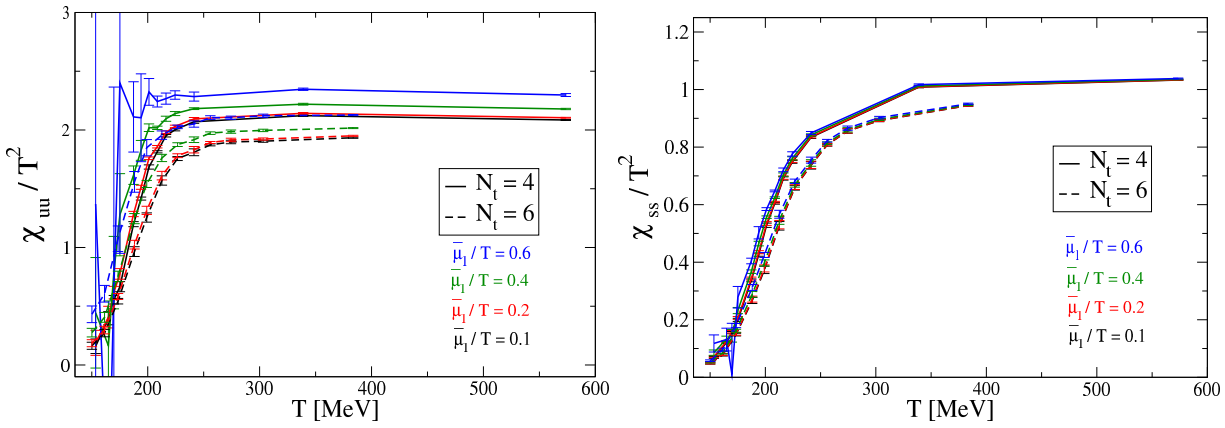

FIG. 7: (Left panel) The light-light quark number susceptibility *vs.* temperature for several values of $\bar{\mu}_l/T$ (in different colors) and μ_s tuned such that $n_s \approx 0$. At a given N_t, the larger $\bar{\mu}_l/T$, the higher the data appears on the plot. However, at low $\bar{\mu}_l/T$ these differences are very small. (Right panel) Same for the strange-strange quark number susceptibility. Here the data dependence on $\bar{\mu}_l/T$ is very weak.

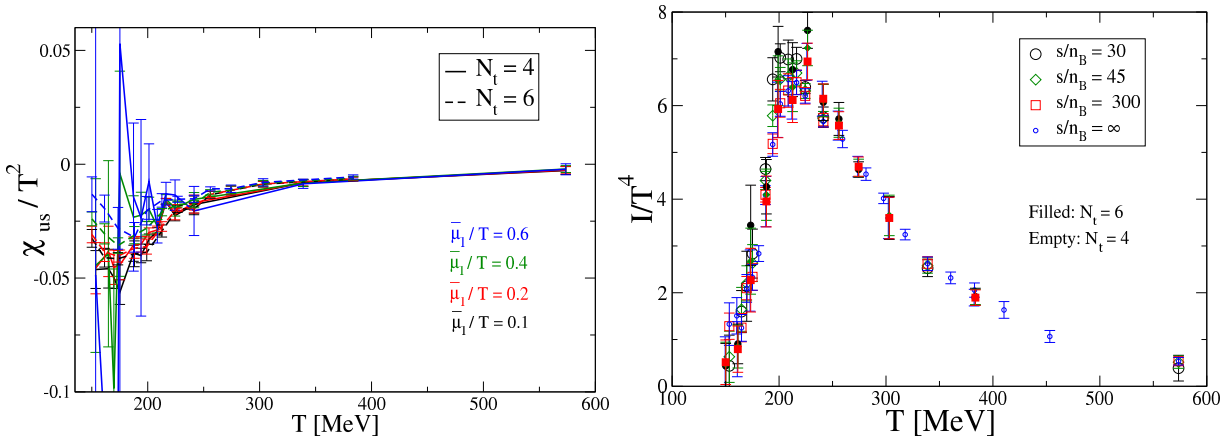

FIG. 8: (Left panel) The light-strange quark number susceptibility *vs.* temperature for several values of $\bar{\mu}_l/T$ (in different colors) and μ_s tuned such that $n_s \approx 0$. As in Fig. 7 (right panel), the data dependence on $\bar{\mu}_l/T$ is very weak. (Right panel) The isentropic interaction measure *vs.* temperature for selected values of s/n_B.

$N_t = 6$ and 4 cases. Indeed, small discretization effects are evident in the isentropic light-light and strange-strange quark number susceptibilities in Figs. 10 (right panel) and 11 (left panel), respectively. However, the isentropic light-quark density, shown in Fig. 10 (left panel), has only marginal discretization effects, despite the fact that it does not have a zeroth order contribution. The large errors on the strange-light susceptibility, shown in Fig. 11 (right panel), precludes us

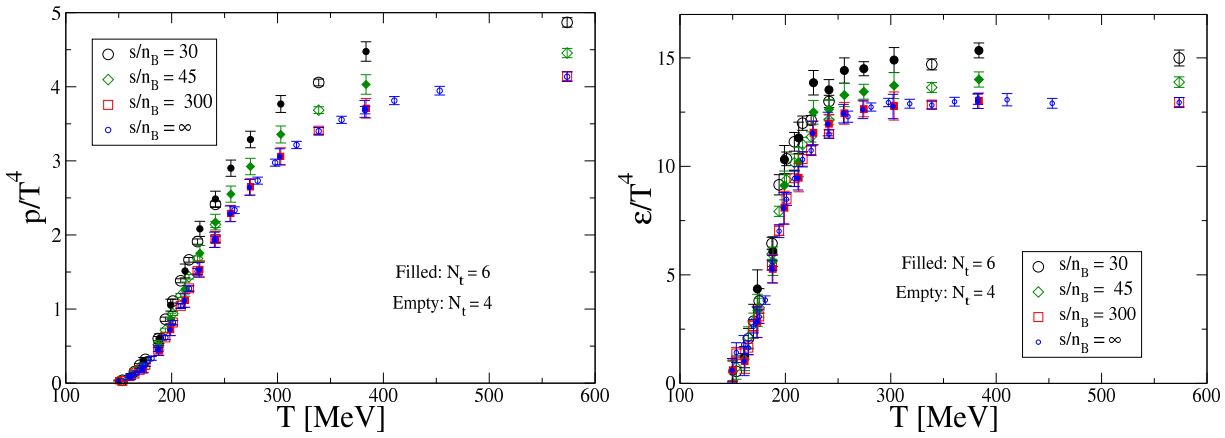

FIG. 9: (Left panel) The isentropic pressure *vs.* temperature for selected values of s/n_B. (Right panel) The same for the isentropic energy density.

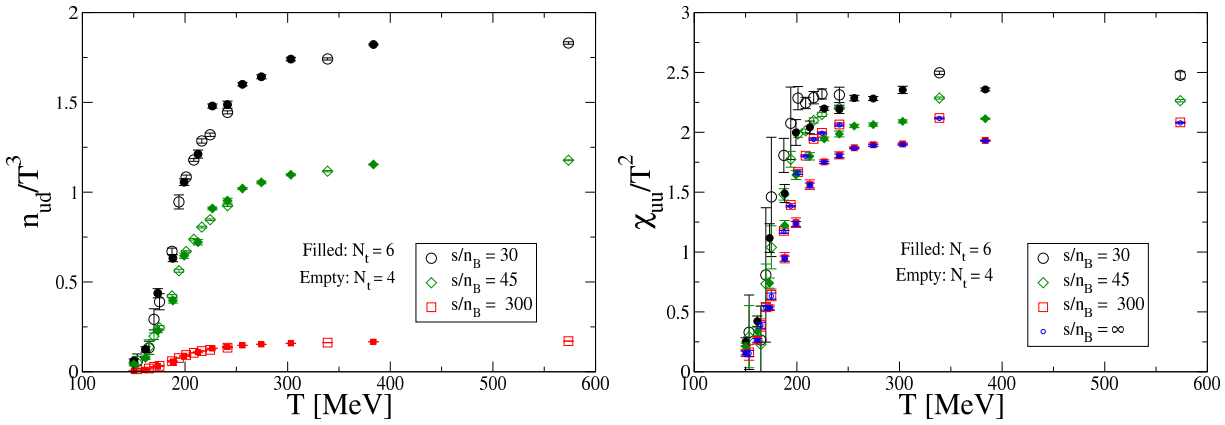

FIG. 10: (Left panel) The isentropic light-quark density *vs.* temperature for selected values of s/n_B. (Right panel) The same for the isentropic light-light quark number susceptibility.

from drawing a conclusion about its discretization effect. To conclude with our final observation, for both values of N_t, we find rather smooth behavior for the isentropic variables indicating that experiments are far from any critical point in the $\mu - T$ plane.

IV. THE EFFECTS OF THE CHARM QUARK ON THE EOS

In this section, we study the effects of the charm quark on the EOS at zero and nonzero chemical potential. Our preliminary results were reported in Ref. [4]. First, let us discuss the relevance of the charm quark contribution. The experiments at RHIC create a "fireball" which thermalizes within $\tau \approx 10^{-24}$ s [8]. The u, d, and s quarks participate in the thermal ensemble describing the

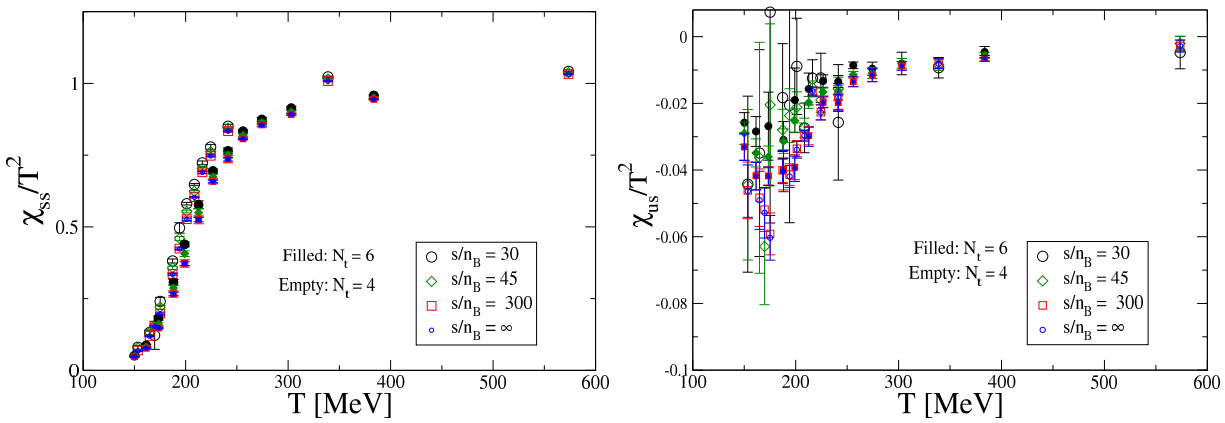

FIG. 11: (Left panel) The isentropic strange-strange quark number susceptibility *vs.* temperature for selected values of s/n_B. (Right panel) The same for the isentropic light-strange quark number susceptibility.

state of the thermalized fireball. Under the experimental conditions, the c quark probably is not thermalized, and thus the 2+1 flavor EOS is considered sufficient for the hydrodynamics models applied to the current experimental data. The question of equilibration of charm, however, is not completely settled as argued, for example, in Ref. [9]. Furthermore, the situation may change for the future LHC experiments. A quark-gluon plasma also existed microseconds after the big bang. Under these primordial conditions and longer time scales, the c quark probably participated in the thermal ensemble as well, which implies that for the study of the early Universe, the EOS with 2+1+1 flavors would be important [10]. For example, the scale factor of the early Universe is affected by the number of quark flavors in the EOS used for its determination [11]. Previously, the question of the charm quark contribution to the EOS at zero chemical potential has been studied on the lattice in Ref. [12] at $N_t = 4$, 6, and 8 using the p4 fermion formulation. That study treated the charm quark as a valence staggered quark. We do the same, but in the asqtad formulation at $N_t = 6$. We tuned the charm quark using a different strategy than in Ref. [12], where the charm quark mass was determined using the η_c or J/Ψ rest mass on all available ensembles. In our study, the charm quark mass was tuned to match the rest mass of the D_s at $\beta = 7.08$ ($a \approx 0.086$ fm) where the discretization effects are smallest on our trajectory. We chose the D_s for our tuning purposes because the discretization effects are smaller for heavy-light mesons than for the heavy-heavy ones [13]. We found $m_c/m_s = 10$ at our tuning point with a 4% uncertainty. We have kept this ratio constant for lower temperatures. It is probably incorrect at the lowest available temperatures, but due to large discretization effects, the tuning is inherently problematic there. Still, we do not expect this to matter much, thanks to the large mass of the c quark and its very small contribution

in that region.

Following our method in Ref. [1] for determining the EOS at zero chemical potential, the 2+1+1 flavor interaction measure was obtained by adding to our previous results for the 2+1 flavor case the charm contribution

$$I_c a^4 = -\frac{1}{4}\left[\frac{d(m_c a)}{d\ln a}\Delta\langle\bar{\psi}\psi\rangle_c + \frac{du_0}{d\ln a}\Delta\left\langle\bar{\psi}\frac{dM}{du_0}\psi\right\rangle_c\right], \tag{3}$$

where the observables in the above are calculated in the heavy-quark-quenched approximation and Δ stands for the difference between the zero and nonzero temperature value of an observable. The mass beta function is approximated as

$$\frac{d(m_c a)}{d\ln a} = 10\frac{d(m_s a)}{d\ln a}, \tag{4}$$

since we kept the ratio $m_c/m_s = 10$ constant along the trajectory. We determined the strange quark mass beta function and the function $du_0/d\ln a$ previously [1]. To find the charm contribution to the pressure and energy density, we integrated Eq. (3) along the physics trajectory, as in Ref. [1] for the 2+1 flavor case.

Again, the nonzero chemical potential calculation was done using the Taylor expansion method, taken to sixth order. For 2+1+1 quark flavors, the Taylor expansion of the pressure is modified to the following form:

$$\frac{p}{T^4} = \sum_{n,m,k=0}^{\infty} c_{nmk}(T)\left(\frac{\bar{\mu}_l}{T}\right)^n\left(\frac{\bar{\mu}_s}{T}\right)^m\left(\frac{\bar{\mu}_c}{T}\right)^k, \tag{5}$$

where $\bar{\mu}_{l,s,c}$ are the chemical potentials in physical units for the light (u,d), strange (s) and charm (c) quarks. Because of CP symmetry the terms in the above are nonzero only if $n+m+k$ is even. The interaction measure has the same form with only $c_{nmk} \to b_{nmk}$. Some details of the explicit calculations for the pressure and interaction measure coefficients can be found in the Appendixes. We used 800 random sources per lattice in the transition region and 400 outside it to calculate the new observables in the expansions of the pressure and interaction measure. For the calculation at nonzero chemical potential, the valence c quark had a low cost in terms of computer time, but it required a sizable software development. For $2+1$ flavors we had 95 observables to code and for $2+1+1$ flavors there were 399.

Turning to our results, let us first examine the effects of the charm quark on the EOS at zero chemical potential. Figure 12 (left panel) shows our results for the EOS with 2+1+1 flavors and compares it with previous results for 2+1 flavors [1]. The charm quark contribution grows with

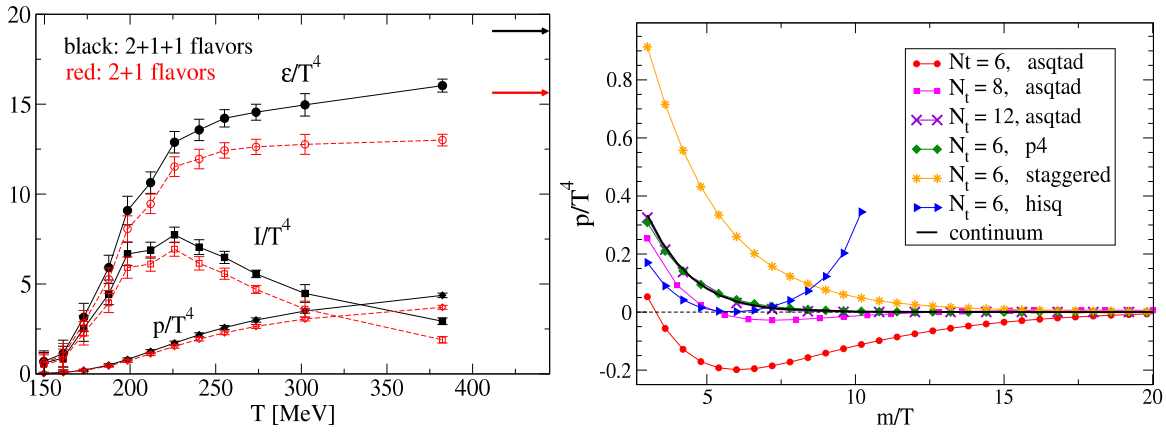

FIG. 12: (Left panel) Interaction measure (I), pressure (p) and energy density (ε) divided by the temperature to the fourth power (T^4) for the cases of 2+1 (red) and 2+1+1 (black) flavors. The arrows indicate the energy density Stefan-Boltzmann limit for both cases. (Right panel) The pressure for 1 quark flavor in the free theory *vs.* the ratio of the quark mass (m) and temperature (T) for different staggered quark formulations. The rise of the pressure at large m/T in the HISQ case shows that higher order corrections to the Naik term are needed in this region. Currently we have corrections up to $O(m^8)$ only.

temperature, as expected, and at the highest available T it contributes about 20% to the energy density. We conclude that in the cases where the charm quark is thermalized, its contribution to the EOS at temperatures higher than about 200 MeV, cannot be ignored. Our result at $N_t = 6$ is qualitatively similar to the previous work [12], but quantitatively our charm quark contributions to the energy density and pressure are about 25%-30% lower by comparison at temperatures around 400 MeV. A possible explanation for this is the larger discretization effects for the heavy-quark pressure for the asqtad action than for the p4 action. Figure 12 (right panel) shows the free quark pressure as a function of the ratio of the (heavy) quark mass and the temperature for different staggered lattice fermion formulations. The asqtad action at $N_t = 6$ shows a negative value for the pressure for a range of heavy-quark masses while the p4 action is close to the continuum limit. Our results for the charm contribution to the EOS do not show the outright unphysical behavior occurring in the free quark case, but it is possible that the heavy-quark discretization effects depress the lattice values.

Now let us turn to the results at nonzero chemical potential. Figures 13 and 14 present some of the pressure and interaction measure expansion coefficients which are directly related to the charm quark contribution at nonzero chemical potential. The first row in both figures shows the

unmixed coefficients and the second row—three of the mixed coefficients. The mixed coefficients are quite small and are much noisier than the unmixed ones, which was expected. As a whole, the new unmixed coefficients c_{00n} and b_{00n} in the pressure and interaction measure expansions are small compared with the c_{n00}, c_{0n0}, b_{n00}, and b_{0n0} coefficients. For numerical comparisons see Sec. II, where the latter four sets are defined without the last zero in the subscripts. These new coefficients remain well below the continuum (massless) Stefan-Boltzmann values at the highest temperature available here. This is not surprising, since over our temperature range $T < 2T_c$, the charm quark mass is much larger than the temperature. The first panel of Fig. 13 shows that c_{002} becomes slightly negative for temperatures up to about 220 MeV. This behavior is obviously unphysical, since this coefficient is directly proportional to the necessarily positive charm quark number susceptibility at zero chemical potential $\chi_{cc}(\mu_{l,s,c} = 0) \sim \langle n_c^2 \rangle$, where n_c is the charm quark number density. It follows that c_{002} should be a non-negative number at all temperatures. We tracked this unphysical behavior to the interplay between the heavy-quark mass and the Naik term in the asqtad action. In the tuning of the latter, corrections proportional to m_c^2 were not included. It is easiest to understand this if we examine the quark number susceptibility for free asqtad (Naik) fermions at large quark masses shown in Fig. 15 (left panel). In the continuum limit, this susceptibility should approach zero from above with increasing heavy-quark mass. We find that at $N_t = 6$ and 8 there is a pronounced "dip" into negative values for a certain range of large quark masses. This effect is much smaller at $N_t = 12$. Since this particular discretization effect does not occur for standard staggered fermions at $N_t = 6$, we conclude that certain thermodynamic quantities, such as susceptibilities, are sensitive to the "length" of the Naik term and require large N_t's in order to overcome their unphysical behavior. From Fig. 15 (left panel), the p4 action seems to be much closer to the continuum limit at $N_t = 6$ and very probably will not show this particular discretization effect in the dynamical case. The HISQ action [14] improves the heavy-quark dispersion relation by tuning the coefficient of the Naik term. (The same tuning could have been done with the asqtad action.) Tuning suppresses this unphysical behavior for $N_t \geq 6$ for the range of m/T up to $O(8)$. Still, in our unquenched 2+1 flavor case, the negative dip in the c_{002} coefficient is quite small, so that its effect, for example, on the isentropic EOS is negligible over the parameter range relevant to heavy-ion collisions. Of course, other mixed and unmixed coefficients might be affected by the limited temporal extent $N_t = 6$ as well, but since they are even smaller than c_{002} we can also ignore their unphysical contribution at low temperatures and small chemical potentials.

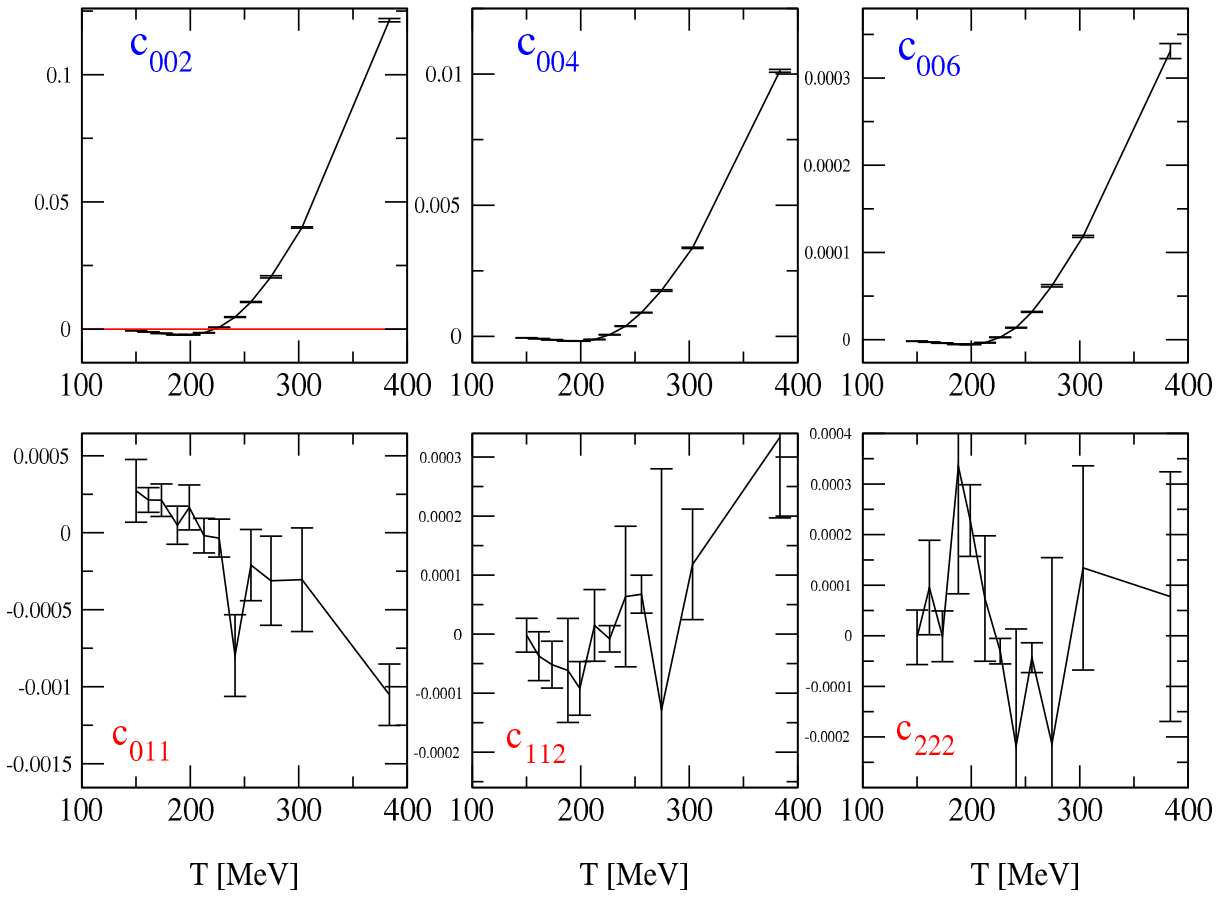

FIG. 13: Some of the new Taylor expansion coefficients for the pressure at nonzero chemical potential when the charm quark is added to the partition function.

From the point of view of the isentropic EOS, our results show that the effect of the charm quark cannot be simply ignored. We have determined the approximate isentropic trajectories in the (μ_l, μ_s, μ_c, T) space, by numerically solving the system

$$\frac{s}{n_B}(\mu_l,\mu_s,\mu_c,T)=C, \qquad \frac{n_s}{T^3}(\mu_l,\mu_s,\mu_c,T)=0, \qquad \frac{n_c}{T^3}(\mu_l,\mu_s,\mu_c,T)=0, \tag{6}$$

with $C = 30$, 45, and 300. Figures 15 (right panel) and 16 (both panels) present the 2+1+1 flavor isentropic interaction measure, pressure, and energy density, respectively, and compare them with the 2+1 flavor case. We see that the charm quark contribution is non-negligible, although it is due mainly to the contribution of the zeroth order coefficients in the Taylor expansions (*i.e.*, the EOS calculated at zero chemical potential). We also note that for the range of temperatures between about 220 and 280 MeV, the errors on the isentropic interaction measure become large. In this region of the isentropic trajectory, μ_c is big enough to make contributions from the quite noisy mixed coefficients visible. The isentropic energy density, of course, inherits this feature, being a

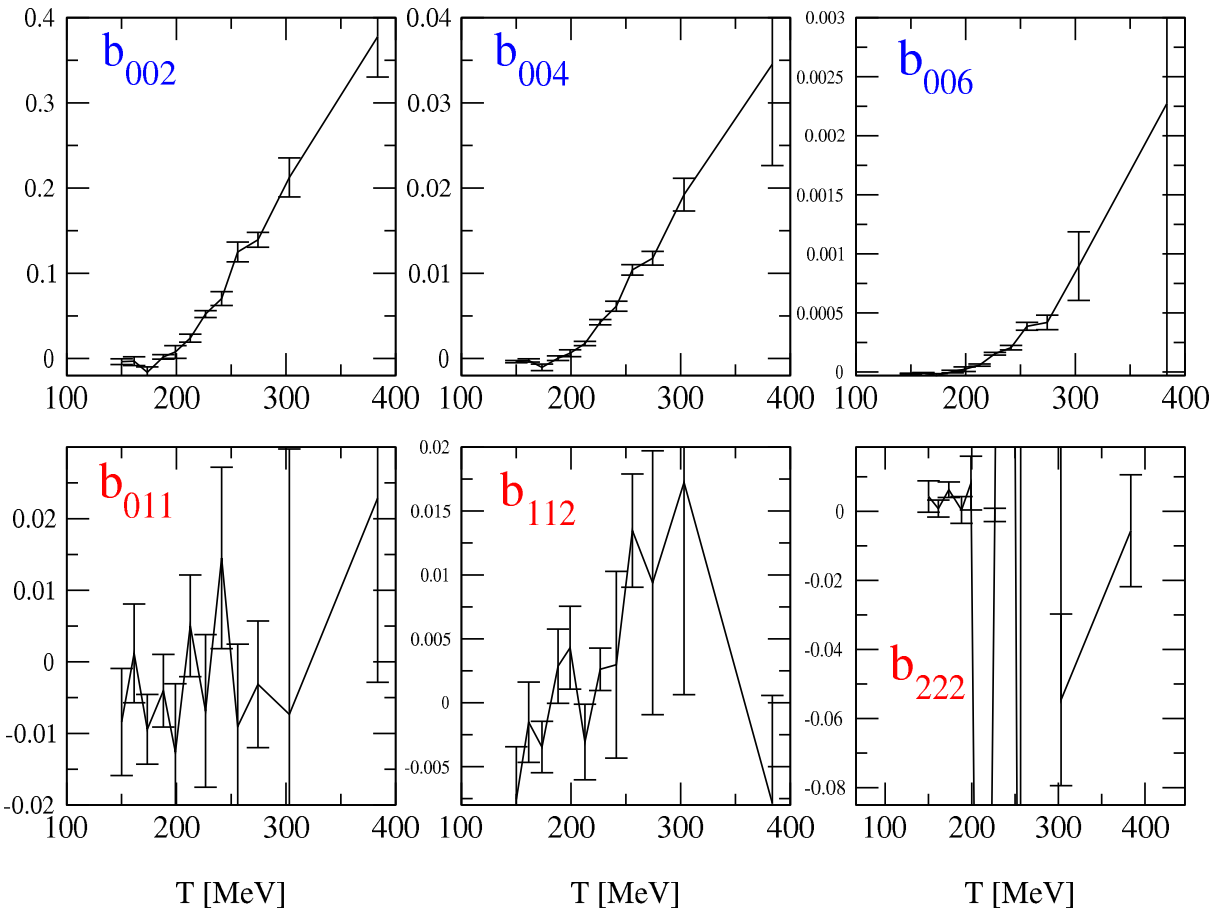

FIG. 14: Some of the new Taylor expansion coefficients for the interaction measure at nonzero chemical potential when the charm quark is added to the partition function.

linear combination of the interaction measure and the pressure.

V. EFFECTS OF THE BOTTOM QUARK ON THE EOS

In the previous section, we presented evidence that the charm quark contributions to the EOS are non-negligible. At still higher temperatures the *b*- and eventually *t*-quark contributions should be similarly non-negligible. In this section, we examine the effects of the bottom quark on the EOS in the range of temperatures up to about 400 MeV. Since the bottom quark is considerably heavier than the charm quark, we expect its contribution to the EOS to be smaller. To estimate it, we simply repeated the charm quark calculation but with a heavier mass corresponding to the bottom quark. The quenching error, even if relevant, will be smaller than the corresponding one for the charm quark. On the ensemble that we used for the charm quark, we tune the bottom quark

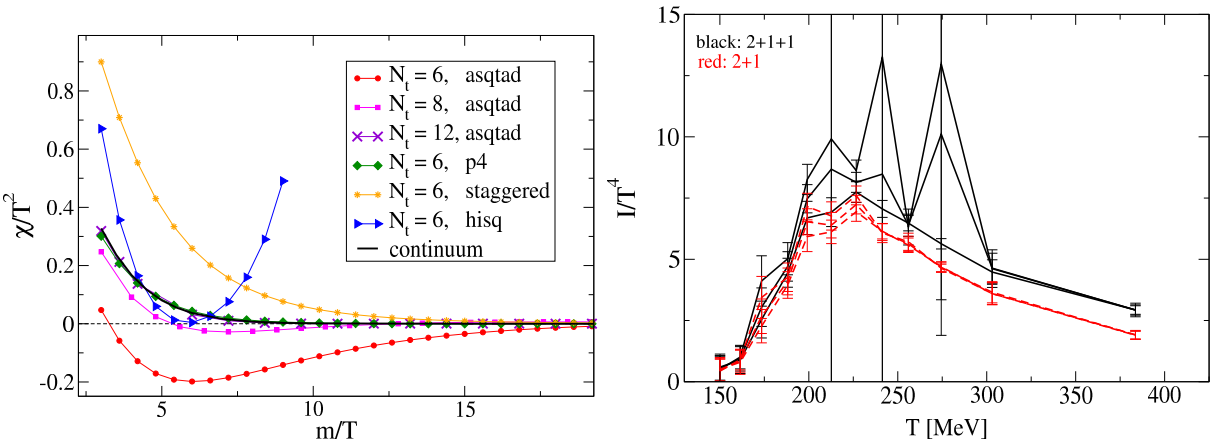

FIG. 15: (Left panel) The quark number susceptibility for 1 quark flavor in the free theory *vs.* the ratio of the quark mass (m) and temperature (T) for different staggered quark formulations. The reason for the rise of the susceptibility in the HISQ case for large m/T is the same as explained in the caption of the right panel of Fig. 12. (Right panel) The isentropic interaction measure at selected s/n_B values for 2+1 and 2+1+1 flavors (red and black respectively). For a data set with the same color (*i.e.*, produced with the same number of quark flavors), the highest lying results are for $s/n_B = 30$, in the middle is the $s/n_B = 45$ case and the case of $s/n_B = 300$ has the lowest lying values.

mass to match the B_s rest mass to its experimental value. We found that within 5% $m_b/m_s = 38$. We kept that ratio constant along the physics trajectory. The problems of the tuning of the bottom quark are potentially worse than in the case of the charm quark, but we do not expect them to skew significantly our final result for the EOS, since the bottom quark contribution itself is expected to be small. Figure 17 (left panel) shows the pressure and energy density at zero chemical potential with $(2+1+1+1)$ and without $(2+1+1)$ the bottom quark. We can conclude that the bottom quark contribution to the EOS at zero chemical potential is small (less than a standard deviation) in the transition region. It grows to about a standard deviation at temperatures close to 400 MeV. However, the range of temperatures we examine here is somewhat limited and probably by $T \sim 600$ MeV the bottom quark effects would grow to be statistically significant for comparable statistics at that temperature. We also have to bear in mind that the heavy-quark discretization effects may play a significant role here and keep the bottom quark contribution lower than what it would be in the continuum limit.

As for the EOS at small nonzero chemical potential, our results for the coefficients of the Taylor series beyond the zeroth order term discussed above show that the bottom quark contribution can

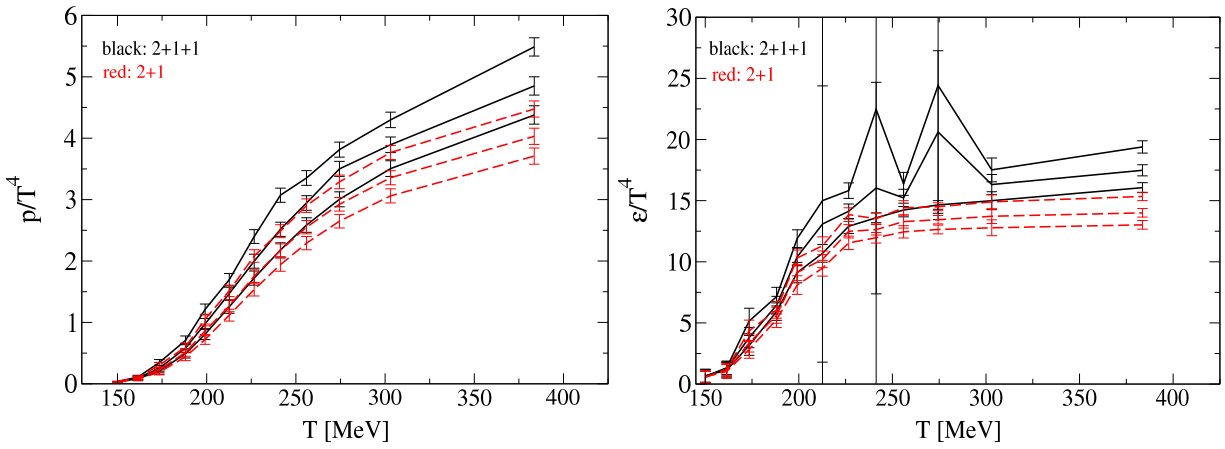

FIG. 16: (Left panel) The isentropic pressure at selected s/n_B values for 2+1 and 2+1+1 flavors (red and black respectively). The data ordering is as in the right pannel of Fig. 15. (Right panel) The same for the isentropic energy density.

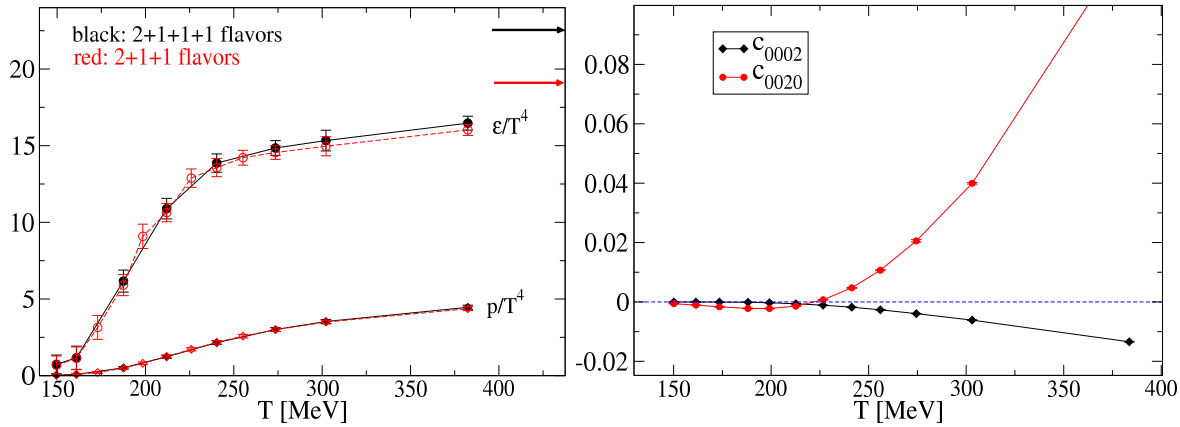

FIG. 17: (Left panel) The pressure and energy density *vs.* temperature for 2+1+1 and 2+1+1+1 flavors (red and black, respectively). The arrows indicate the energy density Stefan-Boltzmann values for both cases. (Right panel) The pressure Taylor expansion coefficients c_{0020} and c_{0002} *vs.* temperature.

be safely ignored at the present level of statistics. The discretization effect which we found for the charm quark in the previous section is much worse for the bottom quark. Figure 17 (right panel) compares the c_{0020} coefficient (referred to as c_{002} in the previous section) and the coefficient c_{0002} in the Taylor expansion for the pressure when all chemical potentials $\mu_{l,s,c,b} \neq 0$. The c_{0002} is persistently negative at all available temperatures. At the present level of statistics and small nonzero chemical potential, this effect is unimportant. But if higher precision is desired, one should tune the coefficient of the Naik term and increase N_t.

VI. CONCLUSIONS

We extended our thermodynamics study of the quark-gluon plasma with chemical potential to finer lattices with temporal extent $N_t = 6$. Comparing our results with previous results at $N_t = 4$ gives an indication of the importance of cutoff effects. As before, we used the Taylor expansion method to sixth order for the case of 2+1 quark flavors. We found small but significant changes in the coefficients of the Taylor expansions of the pressure and interaction measure in going from $N_t = 4$ to 6. This leads to small differences in the resulting interaction measure, pressure, and energy density between the two cases, when matching to the experimental condition of zero strange quark density and keeping $\bar{\mu}_l/T$ constant. Under these conditions, small discretization effects are also visible in the light-light, light-strange and strange-strange quark number susceptibilities and the light-quark density. On the other hand, the isentropic EOS shows very little difference between $N_t = 4$ and 6. More pronounced lattice spacing effects are evident in the isentropic light-light and strange-strange quark number susceptibilities, which we attribute to the fact that these quantities have contributions only from the nonzeroth order Taylor expansion coefficients which are more sensitive to the cutoff. And finally, we did not find any peaks along the isentropic trajectories, which suggests that current experiments operate away from a possible critical point.

A full-flavor quark-gluon plasma EOS is undoubtedly important for cosmological studies. Accordingly, we determined the effects of the charm quark (at zero and nonzero chemical potential) and the bottom quark (at zero chemical potential only) on the EOS. Both heavy quarks were represented in the heavy-quark-quenched approximation by asqtad valence quarks. We expect that the quenching error for such heavy quarks is small, especially for the b quark, but only a direct comparison with a calculation with dynamical c and b quarks can confirm that. We found that the contribution of the charm quark at zero chemical potential reaches about 20% in the energy density at temperatures of about 400 MeV and cannot be ignored in a high-precision cosmological calculation of the properties of the early Universe. The bottom quark contribution is within a standard deviation at that temperature. Our results for the charm and bottom effects on the EOS, however, may be affected by the heavy-quark discretization error we find in the free asqtad action calculation. This implies that they are possibly lower than their respective continuum values.

At nonzero chemical potential, both charm and bottom quarks present a problem (the bottom quark much more so), since we found heavy-quark discretization effects in the Taylor expansion coefficients (especially large for the bottom quark), which could be overcome by tuning the coef-

ficient of the Naik term and/or using $N_t > 6$. However, the charm and bottom quark contributions to the EOS due exclusively to the nonzero chemical potential are very small over the parameter range accessible to heavy-ion collisons, and at our level of precision they are entirely within the present statistical errors of the EOS at zero chemical potential.

ACKNOWLEDGMENTS

This work was supported by the U.S. Department of Energy under grant numbers DE-FC02-06ER-41439, DE-FC02-06ER-41443, DE-FC06-01ER-41437, DE-FG02-04ER-41298, and DE-FG02-91ER-40661 and by the U.S. National Science Foundation under grant numbers OCI08-32315, PHY05-55234, PHY05-55397, PHY07-03296, PHY07-57035, PHY07-57333, PHY07-04171, and PHY09-03536. An allocation of computer time from the Center for High Performance Computing at the University of Utah is gratefully acknowledged. Code development was carried out in part using the computational resources of Indiana University. Computation for this research was supported in part by the U.S. National Science Foundation through TeraGrid resources provided by the Texas Advanced Computing Center (TACC), the Louisiana Optical Network Initiative (LONI), and the National Center for Supercomputing Applications (NCSA) under grant number TG-MCA93S002. Computation for this work was also carried out on the Fermilab LQCD cluster, supported by the Offices of Science, High Energy Physics, and Nuclear Physics of the U.S. Department of Energy.

---

[1] C. Bernard et al., Phys. Rev. **D75**, 094505 (2007) [arXiv:hep-lat/0611031].

[2] C. Bernard et al., Phys. Rev. **D77**, 014503 (2008) [arXiv:0710.1330].

[3] S. Basak et al. (MILC), PoS **LATTICE2008**, 171 (2008) [arXiv:0910.0276].

[4] L. Levkova, PoS **LAT2009**, 170 (2009) [arXiv:0910.3006].

[5] C. R. Allton et al., Phys. Rev. **D66**, 074507 (2002) [arXiv:hep-lat/0204010].

[6] R. V. Gavai and S. Gupta, Phys. Rev. **D68**, 034506 (2003) [arXiv:hep-lat/0303013].

[7] K. Orginos and D. Toussaint (MILC), Phys. Rev. **D59**, 014501 (1998) [arXiv:hep-lat/9805009]; J. F. Lagaë and D. K. Sinclair, Phys. Rev. **D59**, 014511 (1998) [arXiv:hep-lat/9806014]; D. Toussaint and K. Orginos (MILC) , Nucl. Phys. B, Proc. Suppl. **73**, 909 (1999) [arXiv:hep-lat/9809148];

G. P. Lepage, Phys. Rev. **D59**, 074502 (1999) [arXiv:hep-lat/9809157]; K. Orginos, R. Sugar, and D. Toussaint, Nucl. Phys. B, Proc. Suppl. **83**, 878 (2000) [arXiv:hep-lat/9909087].

[8] K. Adcox et al. (PHENIX), Nucl. Phys. **A757**, 184 (2005) [arXiv:nucl-ex/0410003].

[9] M. Laine, PoS **LAT2009**, 006 (2009) [arXiv:0910.5168].

[10] M. Laine and Y. Schröder, Phys. Rev. **D73**, 085009 (2006) [arXiv:hep-ph/0603048].

[11] Michael McGuigan and Wolfgang Söldner [arXiv:0810.0265].

[12] M. Cheng (RBC-Bielefeld), PoS **LAT2007**, 173 (2007) [arXiv:0710.4357]; "The QCD equation of state with charm quarks from lattice QCD", Ph.D. thesis, Collumbia University (2008).

[13] A. S. Kronfeld, Nucl. Phys. B, Proc. Suppl. **53**, 401 (1997) [arXiv:hep-lat/9608139].

[14] E. Follana et al. (HPQCD Collaboration and UKQCD Collaboration), Phys. Rev. **D75**, 054502 (2007) [arXiv:hep-lat/0610092].

Appendix A: General framework for adding the charm quark to the EOS at nonzero chemical potential

With the addition of the charm quark to the u, d and s quarks in the sea, the partition function becomes:

$$\mathcal{Z} = \int \mathcal{D}U\, e^{\frac{n_l}{4}\ln\det\mathcal{M}_l} e^{\frac{n_s}{4}\ln\det\mathcal{M}_s} e^{\frac{n_c}{4}\ln\det\mathcal{M}_c} e^{-S_g}, \tag{A1}$$

with $\mathcal{M}_f$ being the quark matrix for flavor f. Thus, the pressure can be now expanded in the following manner:

$$\frac{p}{T^4} = \sum_{n,m,k=0}^{\infty} c_{nmk}(T) \left(\frac{\bar{\mu}_l}{T}\right)^n \left(\frac{\bar{\mu}_s}{T}\right)^m \left(\frac{\bar{\mu}_c}{T}\right)^k, \tag{A2}$$

where $\bar{\mu}_f$ is the quark chemical potential for flavor f and the coefficients are

$$c_{nmk}(T) = \frac{1}{n!}\frac{1}{m!}\frac{1}{k!}\frac{N_\tau^3}{N_\sigma^3}\frac{\partial^{n+m+k}\ln\mathcal{Z}}{\partial(\mu_l N_\tau)^n \partial(\mu_s N_\tau)^m \partial(\mu_c N_\tau)^k}\Big|_{\mu_{l,s,c}=0}, \tag{A3}$$

with μ_f is the quark chemical potential in lattice units. The coefficients above are nonzero only if $n+m+k$ is even. A similar expansion applies to the interaction measure. These coefficients are for the asqtad quark action:

$$b_{nmk} = -\frac{1}{n!m!k!}\frac{N_t^3}{N_s^3}\sum_{f=l,s,c}\frac{n_f}{4}\left[\frac{d(m_f a)}{d\ln a}\Big|_{\mu_{l,s,c}=0} \mathrm{tr}\,\frac{\partial^{n+m+k}\langle 2M_f^{-1}\rangle}{\partial(\mu_l N_t)^n \partial(\mu_s N_t)^m \partial(\mu_c N_t)^k}\right|_{\mu_{l,s,c}=0}$$

$$+\left.\frac{du_0}{d\ln a}\right|_{\mu_{l,s,c}=0}\mathrm{tr}\,\frac{\partial^{n+m+k}\langle M_f^{-1}\frac{dM_f}{du_0}\rangle}{\partial(\mu_l N_t)^n\partial(\mu_s N_t)^m\partial(\mu_c N_t)^k}\Bigg|_{\mu_{l,s,c}=0}\Bigg]$$
$$-\frac{1}{n!m!k!}\frac{N_t^3}{N_s^3}\left.\frac{\partial^{n+m+k}\langle\,\mathcal{G}\,\rangle}{\partial(\mu_l N_t)^n\partial(\mu_s N_t)^m\partial(\mu_c N_t)^k}\right|_{\mu_{l,s,c}=0}. \tag{A4}$$

In the above, $\mathcal{G}=-dS_g/d\ln a$, with S_g being the gluon part of the action.

Appendix B: Calculating the pressure coefficients in the Taylor expansion

These are most easily calculated using the following (similar to the derivation in the Appendix in Ref. [2]):

$$\frac{\partial\ln Z}{\partial\mu_l} \equiv \mathcal{A}_{100}=\langle L_1\rangle, \tag{B1}$$
$$\frac{\partial\ln Z}{\partial\mu_s} \equiv \mathcal{A}_{010}=\langle H_1\rangle, \tag{B2}$$
$$\frac{\partial\ln Z}{\partial\mu_c} \equiv \mathcal{A}_{001}=\langle Q_1\rangle. \tag{B3}$$

It can be shown that

$$\frac{\partial\mathcal{A}_{nmk}}{\partial\mu_l} = \mathcal{A}_{n+1,m,k}-\mathcal{A}_{100}\mathcal{A}_{nmk}, \tag{B4}$$
$$\frac{\partial\mathcal{A}_{nmk}}{\partial\mu_s} = \mathcal{A}_{n,m+1,k}-\mathcal{A}_{010}\mathcal{A}_{nmk}, \tag{B5}$$
$$\frac{\partial\mathcal{A}_{nmk}}{\partial\mu_c} = \mathcal{A}_{n,m,k+1}-\mathcal{A}_{001}\mathcal{A}_{nmk}, \tag{B6}$$

where

$$\mathcal{A}_{nmk}\equiv\left\langle e^{-L_0}e^{-H_0}e^{-Q_0}\frac{\partial^n e^{L_0}}{\partial\mu_l^n}\frac{\partial^m e^{H_0}}{\partial\mu_s^m}\frac{\partial^k e^{Q_0}}{\partial\mu_c^k}\right\rangle. \tag{B7}$$

In all of the above, Q_k is defined as:

$$Q_k=\frac{n_c}{4}\frac{\partial^k\ln\det M_c}{\partial\mu_c^k}. \tag{B8}$$

The operators L_k and H_k have a similar form for the light and the strange quark respectively. All coefficients c_{nmk} which have at least one of the indices equal to zero have the same form as in the Appendix of Ref. [2], with appropriate substitutions of L_n or H_n with Q_k. The "new" coefficients that appear to $O(6)$ are $c_{(2,1,1)}$, $c_{(3,2,1)}$, c_{222} and $c_{(4,1,1)}$, where the notation (m,n,k) means all

distinct permutations of the indices. Explicitly we have

$$c_{211} = \frac{1}{2!1!1!}\frac{1}{N_s^3 N_t}(\mathcal{A}_{211} - 2\mathcal{A}_{110}\mathcal{A}_{101} - \mathcal{A}_{011}\mathcal{A}_{200}), \tag{B9}$$

$$c_{222} = \frac{1}{2!2!2!}\frac{1}{N_s^3 N_t^3}(\mathcal{A}_{222} + 16\mathcal{A}_{110}\mathcal{A}_{101}\mathcal{A}_{011} + 4\mathcal{A}_{101}^2\mathcal{A}_{020} + 4\mathcal{A}_{011}^2\mathcal{A}_{200} + 4\mathcal{A}_{110}^2\mathcal{A}_{002} + 2\mathcal{A}_{002}\mathcal{A}_{200}\mathcal{A}_{020}$$
$$-\mathcal{A}_{002}\mathcal{A}_{220} - \mathcal{A}_{200}\mathcal{A}_{022} - \mathcal{A}_{202}\mathcal{A}_{020} - 4\mathcal{A}_{101}\mathcal{A}_{121} - 4\mathcal{A}_{110}\mathcal{A}_{112} - 4\mathcal{A}_{011}\mathcal{A}_{211}), \tag{B10}$$

$$c_{321} = \frac{1}{3!2!1!}\frac{1}{N_s^3 N_t^3}(\mathcal{A}_{321} + 12\mathcal{A}_{110}^2\mathcal{A}_{101} - 6\mathcal{A}_{211}\mathcal{A}_{110} - 2\mathcal{A}_{011}\mathcal{A}_{310} - 3\mathcal{A}_{220}\mathcal{A}_{101} - \mathcal{A}_{020}\mathcal{A}_{301}$$
$$-3\mathcal{A}_{200}\mathcal{A}_{121} + 6\mathcal{A}_{020}\mathcal{A}_{200}\mathcal{A}_{101} + 12\mathcal{A}_{011}\mathcal{A}_{110}\mathcal{A}_{200}), \tag{B11}$$

$$c_{411} = \frac{1}{4!1!1!}\frac{1}{N_s^3 N_t^3}(\mathcal{A}_{411} + 24\mathcal{A}_{110}\mathcal{A}_{101}\mathcal{A}_{200} - 4\mathcal{A}_{301}\mathcal{A}_{110} - 4\mathcal{A}_{101}\mathcal{A}_{310} - \mathcal{A}_{011}\mathcal{A}_{400}$$
$$-6\mathcal{A}_{200}\mathcal{A}_{211} + 6\mathcal{A}_{011}\mathcal{A}_{200}^2). \tag{B12}$$

Permuting the indices above gives us the rest of the coefficients. Calculating the $\mathcal{A}_{nmk}$ is straightforward from Eq. (B7).

Appendix C: Calculating the interaction measure coefficients in the Taylor expansion

1. First type of derivative

This section gives a method to calculate the derivative:

$$\left.\frac{\partial^{n+m+k}\langle M_f^{-1}\rangle}{\partial(\mu_l N_t)^n \partial(\mu_s N_t)^m \partial(\mu_c N_t)^k}\right|_{\mu_{l,s,c}=0}, \tag{C1}$$

for $f = l,s,c$, when all of the indices n,m and k are nonzero. See Ref. [2] for results when at least one is zero. It is convenient to define the observables:

$$\mathcal{B}_{nmk} \equiv \left\langle \mathrm{e}^{-L_0}\mathrm{e}^{-H_0}\mathrm{e}^{-Q_0}\frac{\partial^n(\mathrm{tr}\, M_l^{-1}\mathrm{e}^{L_0})}{\partial\mu_l^n}\frac{\partial^m \mathrm{e}^{H_0}}{\partial\mu_s^m}\frac{\partial^k \mathrm{e}^{Q_0}}{\partial\mu_c^k}\right\rangle, \tag{C2}$$

$$\mathcal{B}'_{nmk} \equiv \left\langle \mathrm{e}^{-L_0}\mathrm{e}^{-H_0}\mathrm{e}^{-Q_0}\frac{\partial^n \mathrm{e}^{L_0}}{\partial\mu_l^n}\frac{\partial^m(\mathrm{tr}\, M_s^{-1}\mathrm{e}^{H_0})}{\partial\mu_s^m}\frac{\partial^k \mathrm{e}^{Q_0}}{\partial\mu_c^k}\right\rangle, \tag{C3}$$

$$\mathcal{B}''_{nmk} \equiv \left\langle \mathrm{e}^{-L_0}\mathrm{e}^{-H_0}\mathrm{e}^{-Q_0}\frac{\partial^n \mathrm{e}^{L_0}}{\partial\mu_l^n}\frac{\partial^m \mathrm{e}^{H_0}}{\partial\mu_s^m}\frac{\partial^k(\mathrm{tr}\, M_c^{-1}\mathrm{e}^{Q_0})}{\partial\mu_c^k}\right\rangle. \tag{C4}$$

The above means:

$$\mathcal{B}_{000} \equiv \left\langle \mathrm{tr}\, M_l^{-1}\right\rangle, \tag{C5}$$

$$\mathcal{B}'_{000} \equiv \left\langle \mathrm{tr}\, M_s^{-1}\right\rangle, \tag{C6}$$

$$\mathcal{B}''_{000} \equiv \left\langle \mathrm{tr}\, M_c^{-1}\right\rangle. \tag{C7}$$

Let $f = l$ then we have the following rule:

$$\frac{\partial \mathcal{B}_{nmk}}{\partial \mu_l} = \mathcal{B}_{n+1,mk} - \mathcal{A}_{100}\mathcal{B}_{nmk}, \tag{C8}$$

$$\frac{\partial \mathcal{B}_{nmk}}{\partial \mu_s} = \mathcal{B}_{n,m+1,k} - \mathcal{A}_{010}\mathcal{B}_{nmk}, \tag{C9}$$

$$\frac{\partial \mathcal{B}_{nmk}}{\partial \mu_c} = \mathcal{B}_{nm,k+1} - \mathcal{A}_{001}\mathcal{B}_{nmk}. \tag{C10}$$

Using the above, we calculate:

$$\begin{aligned}
\frac{\partial^4 \left\langle \mathrm{tr} M_l^{-1} \right\rangle}{\partial^2 \mu_l \partial \mu_s \partial \mu_c} &= \mathcal{B}_{211} + 2\mathcal{B}_{000}\mathcal{A}_{011}\mathcal{A}_{200} - \mathcal{B}_{000}\mathcal{A}_{211} + 4\mathcal{B}_{000}\mathcal{A}_{110}\mathcal{A}_{101} - \mathcal{A}_{011}\mathcal{B}_{200} \\
&\quad -2\mathcal{B}_{101}\mathcal{A}_{110} - 2\mathcal{B}_{110}\mathcal{A}_{101} - \mathcal{B}_{011}\mathcal{A}_{200}, \qquad \text{(C11)} \\
\frac{\partial^6 \left\langle \mathrm{tr} M_l^{-1} \right\rangle}{\partial^2 \mu_l \partial^2 \mu_s \partial^2 \mu_c} &= \mathcal{B}_{222} - \mathcal{B}_{000}\mathcal{A}_{222} + 2\mathcal{A}_{002}\mathcal{A}_{200}\mathcal{B}_{020} + 2\mathcal{A}_{002}\mathcal{B}_{200}\mathcal{A}_{020} + 2\mathcal{B}_{002}\mathcal{A}_{200}\mathcal{A}_{020} \\
&\quad -4\mathcal{A}_{011}\mathcal{B}_{211} - 4\mathcal{B}_{112}\mathcal{A}_{110} - 4\mathcal{A}_{101}\mathcal{B}_{121} - \mathcal{B}_{002}\mathcal{A}_{220} - \mathcal{B}_{200}\mathcal{A}_{022} - \mathcal{A}_{202}\mathcal{B}_{020} \\
&\quad +16\mathcal{A}_{011}\mathcal{A}_{101}\mathcal{B}_{110} + 16\mathcal{A}_{011}\mathcal{B}_{101}\mathcal{A}_{110} + 16\mathcal{B}_{011}\mathcal{A}_{101}\mathcal{A}_{110} \\
&\quad +8\mathcal{B}_{000}\mathcal{A}_{211}\mathcal{A}_{011} + 8\mathcal{B}_{000}\mathcal{A}_{101}\mathcal{A}_{121} + 8\mathcal{B}_{000}\mathcal{A}_{110}\mathcal{A}_{112} \\
&\quad +8\mathcal{B}_{101}\mathcal{A}_{101}\mathcal{A}_{020} + 8\mathcal{A}_{002}\mathcal{A}_{110}\mathcal{B}_{110} + 8\mathcal{A}_{011}\mathcal{A}_{200}\mathcal{B}_{011} \\
&\quad +2\mathcal{B}_{000}\mathcal{A}_{202}\mathcal{A}_{020} + 2\mathcal{A}_{002}\mathcal{B}_{000}\mathcal{A}_{220} + 2\mathcal{B}_{000}\mathcal{A}_{200}\mathcal{A}_{022} \\
&\quad -12\mathcal{A}_{002}\mathcal{B}_{000}\mathcal{A}_{110}^2 - 12\mathcal{B}_{000}\mathcal{A}_{200}\mathcal{A}_{011}^2 - 12\mathcal{B}_{000}\mathcal{A}_{101}^2\mathcal{A}_{020} \\
&\quad -\mathcal{A}_{002}\mathcal{B}_{220} - \mathcal{A}_{200}\mathcal{B}_{022} - \mathcal{B}_{202}\mathcal{A}_{020} - 4\mathcal{B}_{101}\mathcal{A}_{121} - 4\mathcal{B}_{110}\mathcal{A}_{112} - 4\mathcal{B}_{011}\mathcal{A}_{211} \\
&\quad +4\mathcal{B}_{002}\mathcal{A}_{110}^2 + 4\mathcal{A}_{011}^2\mathcal{B}_{200} + 4\mathcal{A}_{101}^2\mathcal{B}_{020} \\
&\quad -6\mathcal{A}_{002}\mathcal{B}_{000}\mathcal{A}_{200}\mathcal{A}_{020} - 48\mathcal{B}_{000}\mathcal{A}_{110}\mathcal{A}_{011}\mathcal{A}_{101}, \qquad \text{(C12)} \\
\frac{\partial^6 \left\langle \mathrm{tr} M_l^{-1} \right\rangle}{\partial^3 \mu_l \partial^2 \mu_s \partial^1 \mu_c} &= \mathcal{B}_{321} - \mathcal{B}_{000}\mathcal{A}_{321} + 12\mathcal{A}_{110}\mathcal{A}_{011}\mathcal{B}_{200} + 6\mathcal{B}_{000}\mathcal{A}_{220}\mathcal{A}_{101} + 12\mathcal{B}_{110}\mathcal{A}_{011}\mathcal{A}_{200} \\
&\quad -36\mathcal{B}_{000}\mathcal{A}_{110}^2\mathcal{A}_{101} + 12\mathcal{B}_{011}\mathcal{A}_{200}\mathcal{A}_{110} + 6\mathcal{A}_{020}\mathcal{A}_{200}\mathcal{B}_{101} + 24\mathcal{B}_{110}\mathcal{A}_{101}\mathcal{A}_{110} \\
&\quad -6\mathcal{A}_{110}\mathcal{B}_{211} - 3\mathcal{B}_{200}\mathcal{A}_{121} + 2\mathcal{B}_{000}\mathcal{A}_{020}\mathcal{A}_{301} + 12\mathcal{A}_{110}^2\mathcal{B}_{101} + 12\mathcal{B}_{000}\mathcal{A}_{110}\mathcal{A}_{211} \\
&\quad -3\mathcal{A}_{220}\mathcal{B}_{101} + 6\mathcal{B}_{000}\mathcal{A}_{200}\mathcal{A}_{121} - 6\mathcal{A}_{211}\mathcal{B}_{110} - 3\mathcal{B}_{220}\mathcal{A}_{101} - 2\mathcal{B}_{011}\mathcal{A}_{310} \\
&\quad -\mathcal{A}_{020}\mathcal{B}_{301} - \mathcal{B}_{020}\mathcal{A}_{301} - 36\mathcal{A}_{011}\mathcal{B}_{000}\mathcal{A}_{110}\mathcal{A}_{200} - 3\mathcal{A}_{200}\mathcal{B}_{121} + 6\mathcal{A}_{020}\mathcal{A}_{101}\mathcal{B}_{200} \\
&\quad -18\mathcal{A}_{020}\mathcal{B}_{000}\mathcal{A}_{200}\mathcal{A}_{101} + 4\mathcal{A}_{011}\mathcal{B}_{000}\mathcal{A}_{310} + 6\mathcal{A}_{101}\mathcal{B}_{020}\mathcal{A}_{200} - 2\mathcal{A}_{011}\mathcal{B}_{310}, \qquad \text{(C13)} \\
\frac{\partial^6 \left\langle \mathrm{tr} M_l^{-1} \right\rangle}{\partial^4 \mu_l \partial^1 \mu_s \partial^1 \mu_c} &= \mathcal{B}_{411} - \mathcal{B}_{000}\mathcal{A}_{411} - \mathcal{B}_{011}\mathcal{A}_{400} - \mathcal{A}_{011}\mathcal{B}_{400} + 24\mathcal{A}_{101}\mathcal{B}_{110}\mathcal{A}_{200} + 24\mathcal{A}_{110}\mathcal{A}_{200}\mathcal{B}_{101} \\
&\quad +12\mathcal{A}_{200}\mathcal{A}_{011}\mathcal{B}_{200} + 24\mathcal{A}_{110}\mathcal{A}_{101}\mathcal{B}_{200} + 12\mathcal{B}_{000}\mathcal{A}_{200}\mathcal{A}_{211}
\end{aligned}$$

$$+8\mathcal{B}_{000}\mathcal{A}_{301}\mathcal{A}_{110}+8\mathcal{A}_{101}\mathcal{B}_{000}\mathcal{A}_{310}-4\mathcal{A}_{101}\mathcal{B}_{310}-4\mathcal{A}_{110}\mathcal{B}_{301}$$
$$-4\mathcal{B}_{110}\mathcal{A}_{301}-4\mathcal{A}_{310}\mathcal{B}_{101}-6\mathcal{A}_{200}\mathcal{B}_{211}-6\mathcal{A}_{211}\mathcal{B}_{200}-72\mathcal{B}_{000}\mathcal{A}_{200}\mathcal{A}_{101}\mathcal{A}_{110}$$
$$+6\mathcal{A}_{200}^2\mathcal{B}_{011}+2\mathcal{B}_{000}\mathcal{A}_{011}\mathcal{A}_{400}-18\mathcal{A}_{011}\mathcal{A}_{200}^2\mathcal{B}_{000}. \quad \text{(C14)}$$

Replacing $\mathcal{B}$ with $\mathcal{B}'$ or $\mathcal{B}''$ in the above, we get the expressions for the derivatives of $\left\langle \mathrm{tr} M_s^{-1} \right\rangle$ or $\left\langle \mathrm{tr} M_c^{-1} \right\rangle$. The explicit forms of $\mathcal{B}_{nmk}$ are easy to deduce from Eq. (C2). To get the $\mathcal{B}'_{nmk}$ or $\mathcal{B}''_{nmk}$ we need to interchange appropriately the three observables:

$$l_n = \frac{\partial^n \mathrm{tr} M_l^{-1}}{\partial \mu_l^n}, \quad \text{(C15)}$$
$$h_n = \frac{\partial^n \mathrm{tr} M_s^{-1}}{\partial \mu_s^n}, \quad \text{(C16)}$$
$$q_n = \frac{\partial^n \mathrm{tr} M_c^{-1}}{\partial \mu_c^n}, \quad \text{(C17)}$$

along with L_n, H_n and Q_n in the explicit forms of $\mathcal{B}_{nmk}$.

2. Second type of derivative

We also need to calculate the derivatives:

$$\left. \frac{\partial^{n+m+k} \langle M_f^{-1} \frac{dM_f}{du_0} \rangle}{\partial(\mu_l N_t)^n \partial(\mu_s N_t)^m \partial(\mu_c N_t)^k} \right|_{\mu_{l,s,c}=0}, \quad \text{(C18)}$$

where again $f = l, s, c$. Similarly to the previous subsection, we define the observables:

$$\mathcal{C}_{nmk} \equiv \left\langle \mathrm{e}^{-L_0}\mathrm{e}^{-H_0}\mathrm{e}^{-Q_0} \frac{\partial^n [\mathrm{tr}\,(M_l^{-1}\frac{dM_l}{du_0})\mathrm{e}^{L_0}]}{\partial \mu_l^n} \frac{\partial^m \mathrm{e}^{H_0}}{\partial \mu_s^m} \frac{\partial^k \mathrm{e}^{Q_0}}{\partial \mu_c^k} \right\rangle, \quad \text{(C19)}$$
$$\mathcal{C}'_{nmk} \equiv \left\langle \mathrm{e}^{-L_0}\mathrm{e}^{-H_0}\mathrm{e}^{-Q_0} \frac{\partial^n \mathrm{e}^{L_0}}{\partial \mu_l^n} \frac{\partial^m [\mathrm{tr}\,(M_s^{-1}\frac{dM_s}{du_0})\mathrm{e}^{H_0}]}{\partial \mu_s^m} \frac{\partial^k \mathrm{e}^{Q_0}}{\partial \mu_c^k} \right\rangle, \quad \text{(C20)}$$
$$\mathcal{C}''_{nmk} \equiv \left\langle \mathrm{e}^{-L_0}\mathrm{e}^{-H_0}\mathrm{e}^{-Q_0} \frac{\partial^n \mathrm{e}^{L_0}}{\partial \mu_l^n} \frac{\partial^m \mathrm{e}^{H_0}}{\partial \mu_s^m} \frac{\partial^k [\mathrm{tr}\,(M_c^{-1}\frac{dM_c}{du_0})\mathrm{e}^{Q_0}]}{\partial \mu_c^k} \right\rangle. \quad \text{(C21)}$$

From the above,

$$\mathcal{C}_{000} \equiv \left\langle \mathrm{tr}\,(M_l^{-1}\frac{dM_l}{du_0}) \right\rangle, \quad \text{(C22)}$$
$$\mathcal{C}'_{000} \equiv \left\langle \mathrm{tr}\,(M_s^{-1}\frac{dM_s}{du_0}) \right\rangle, \quad \text{(C23)}$$
$$\mathcal{C}''_{000} \equiv \left\langle \mathrm{tr}\,(M_c^{-1}\frac{dM_c}{du_0}) \right\rangle. \quad \text{(C24)}$$

Let $f = l$, then it is easy to see that

$$\frac{\partial \mathcal{C}_{nmk}}{\partial \mu_l} = \mathcal{C}_{n+1,mk} - \mathcal{A}_{100}\mathcal{C}_{nmk}, \tag{C25}$$

$$\frac{\partial \mathcal{C}_{nmk}}{\partial \mu_s} = \mathcal{C}_{n,m+1,k} - \mathcal{A}_{010}\mathcal{C}_{nmk}, \tag{C26}$$

$$\frac{\partial \mathcal{C}_{nmk}}{\partial \mu_c} = \mathcal{C}_{nm,k+1} - \mathcal{A}_{001}\mathcal{C}_{nmk}. \tag{C27}$$

Similar expressions apply in the case of $\mathcal{C}'_{nmk}$ and $\mathcal{C}''_{nmk}$. Then the derivatives

$$\frac{\partial^n \left\langle \mathrm{tr}\,(M^{-1}_{l,s,c}\frac{dM_{l,s}}{du_0}) \right\rangle}{\partial \mu^n_{l,s,c}} \tag{C28}$$

have the form of the derivatives of $\left\langle \mathrm{tr}\,(M^{-1}_{l,s,c}) \right\rangle$ in the previous section with the substitutions $\mathcal{B}_{nmk} \to \mathcal{C}_{nmk}$, $\mathcal{B}'_{nmk} \to \mathcal{C}'_{nmk}$ and $\mathcal{B}''_{nmk} \to \mathcal{C}''_{nmk}$. The explicit forms of $\mathcal{C}_{nmk}$, $\mathcal{C}'_{nmk}$ and $\mathcal{C}''_{nmk}$ are the same as for $\mathcal{B}_{nmk}$, $\mathcal{B}'_{nmk}$ and $\mathcal{B}''_{nmk}$ with the substitutions $l_n \to \lambda_n$, $h_n \to \chi_n$ and $q_n \to \eta_n$ where

$$\lambda_n = \frac{\partial^n \mathrm{tr}\,(M_l^{-1}\frac{dM_l}{du_0})}{\partial \mu_l^n}, \tag{C29}$$

$$\chi_n = \frac{\partial^n \mathrm{tr}\,(M_s^{-1}\frac{dM_s}{du_0})}{\partial \mu_s^n}, \tag{C30}$$

$$\eta_n = \frac{\partial^n \mathrm{tr}\,(M_c^{-1}\frac{dM_c}{du_0})}{\partial \mu_c^n}. \tag{C31}$$

3. Third type of derivative

The last type of derivative that we need is the gauge derivative

$$\left.\frac{\partial^{n+m+k}\langle\, \mathcal{G}\,\rangle}{\partial(\mu_l N_t)^n \partial(\mu_s N_t)^m \partial(\mu_c N_t)^k}\right|_{\mu_{l,s,c}=0}. \tag{C32}$$

In this case, let

$$G_{nmk} \equiv \left\langle \mathcal{G}\ \mathrm{e}^{-L_0}\mathrm{e}^{-H_0}\mathrm{e}^{-Q_0}\frac{\partial^n \mathrm{e}^{L_0}}{\partial \mu_l^n}\frac{\partial^m \mathrm{e}^{H_0}}{\partial \mu_s^m}\frac{\partial^p \mathrm{e}^{Q_0}}{\partial \mu_c^k} \right\rangle, \tag{C33}$$

and similarly as before

$$\frac{\partial G_{nmk}}{\partial \mu_l} = G_{n+1,mk} - \mathcal{A}_{100}G_{nmk}, \tag{C34}$$

$$\frac{\partial G_{nmk}}{\partial \mu_s} = G_{n,m+1,k} - \mathcal{A}_{010}G_{nmk}, \tag{C35}$$

$$\frac{\partial G_{nmk}}{\partial \mu_c} = G_{nm,k+1} - \mathcal{A}_{001}G_{nmk}, \tag{C36}$$

with

$$G_{000} = \langle \mathcal{G} \rangle. \tag{C37}$$

This means that the necessary derivatives $\frac{\partial^{n+m+k}\langle \mathcal{G} \rangle}{\partial(\mu_l N_t)^n \partial(\mu_s N_t)^m \partial(\mu_c N_t)^k}\Big|_{\mu_{l,s,c}=0}$ have the same form as the derivatives $\frac{\partial^{n+m+k}\mathrm{tr}\langle M_f^{-1} \rangle}{\partial(\mu_l N_t)^n \partial(\mu_s N_t)^m \partial(\mu_c N_t)^k}\Big|_{\mu_{l,s,c}=0}$ with $\mathcal{B}_{nmk} \to G_{nmk}$. The G_{nmk} observables have very similar form to the $\mathcal{A}_{nmk}$ observables, but with an additional multiplication by $\mathcal{G}$ inside the ensemble average brackets of each term in them.